Instantaneous stress state of the lithosphere of Southern California: A synthesis of geophysical and compositional products of SCEC

Lajhon Campbell[1] Siyuan Sui[1], Alireza Bahadori[2], Weisen Shen[1], William E. Holt[1]
[1]Stony Brook University, [2]Columbia University

Stony Brook University

SCEC an NSF+USGS center

SB GEOS Stony Brook Center for Geodynamics & Seismology

Introduction

The complex tectonic setting and fault system in California have produced a mosaic of crustal blocks for which their strength varies significantly across the region.

Here we show the chemical, one of the most significant factors that determine crustal strength, can be quantified from a new map of Vp/Vs for the crystalline crust by applying a newly developed data processing scheme that involves a 2-layer H-k stacking of receiver functions. Precisely determining the crustal Vp/Vs will provide us insights of the chemical composition, especially SiO_2 wt% , the oxide that alter the rock elastic and theological properties significantly (Lowry and Pérez-Gussinyé,2011). We test the dynamic effects of the derived compositional structure in a 3-D thermomechanical model.

.

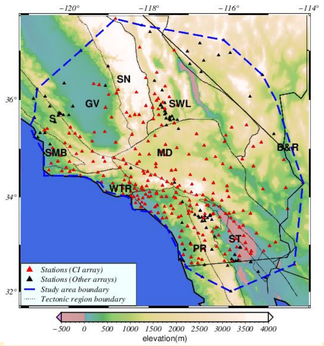

Figure. 1 *The locations of seismic stations used in this study and the corresponding study region are plotted on the topography map (ETOPO1, Amante and Eakins, 2009). 271 stations belonging to Southern California Seismic Network (CI array) and 102 stations from other seismic arrays are plotted in red and black triangles, respectively. The boundary of our study region is outlined by the dashed blue lines. Solid black lines are the state boundaries and dotted black lines mark the boundaries of major tectonic regions in Southern California. Abbreviations: SN (Sierra Nevada), GV (Great Valley), SWL (Southern Walker Lane), S (Salinia), SMB (Santa Maria Basin), MD (Mojave Desert), B&R (Basin and Ranges), WTR (Western Transverse Ranges), PR (Peninsular Ranges), ST (Salton Troughs).*

Data

Event: Magnitude> 5.5, 2010.01.01~2020.01.01
Station: 460 CI stations (265 broadband, 195 strong motion), 148 None CI stations
Method: 2-layer H-κ sequential stacking method (Yeck et al.,2013)

2-layer H-κ stacking

A 2-stage application of the 2-layer H-k stacking is performed here. First, we apply this method to high frequency receiver functions and calculate the thickness and Vp/Vs of the sediment layer. These results are used to eliminate the influence of the reverberations generated by sediment layer in the low frequency receiver functions. Besides the widely used energy stacking (Zhu & Kanamori 2000), the statistic values from individual events are used to estimate the thickness and Vp/Vs (Fig 2).

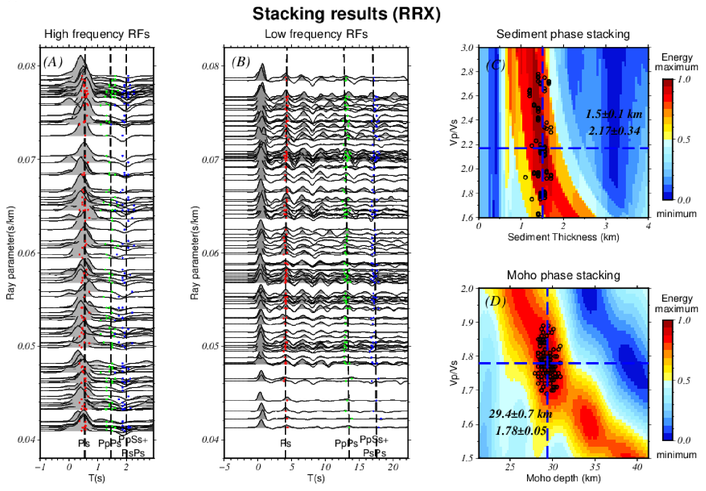

Figure 2: *H-κ stacking results at station CI_RRX (A) High frequency P-wave RFs at station RRX are plotted according to ray parameters. The red, green and blue dots mark the arrival times of Ps, PpPs, PpSs+PsPs phases at sediment bottom, respectively. The dashed lines indicate the predicted arrival times from H-κ energy stacking. (B) Low frequency P-wave RFs. The colored dots mark the arrival times of converted/reverberated phases at the Moho. (C, D) H-κ stacking energy of sediment phases and Moho phases, respectively. The stacked energy from all the RF waveforms is shown by background color, and individual RF predicted results are plotted in circles. The intersections of dashed lines are the mean values of the circles, which are labeled together with the standard deviations..*

Moho depth and Crustal Vp/Vs

Fig.3 shows thickness and Vp/Vs for the sediments at 309 stations and for the crystalline crust at 270 stations as well as the smoothed maps in the background

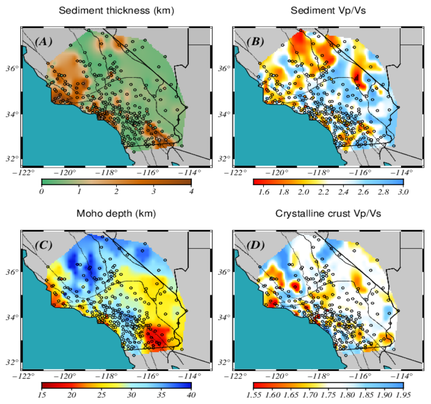

Figure. 3. *(A) Sediment thickness map. Small circles and their colors represent the location and the sediment thickness of each station. (B) Sediment Vp/Vs. (C) Moho depth. (D) Crystalline crust Vp/Vs.*

From Vp/Vs to SiO_2 wt%

By combining the Vp/Vs ratios with a high-resolution Vs model (CVM-H version 6.2), a 1-D SiO_2 wt% model beneath each station in this study can be constructed based on relationship revealed from the petrology database (Hacker et al. 2015, Christensen 1996, Fig. 4).

Figure. 4 *The panel on the left shows a Vs profile increasing with depth. The surface in the middle shows the relationship between SiO2 weight percentage, Vp/Vs, and Vs. Petrology observations: small circles - Hacker et al. 2015; Squares - Christensen 1996. The background color represents the interpolated SiO_2 wt% of the individual rock samples. A clear trend emerges that felsic rocks generally have low Vs and Vp/Vs, while the mafic rocks are on the other side of the spectrum. The panel on the right show the sio2 wt% profile predicted from the Vs profile and Vp/Vs value and how the crust is divided into mafic (M), intermediate (I) and felsic (F) layers.*

Geodynamic Modelling

We use the seismically defined structure described above and a thermal model to develop a 3-D coupled thermo-mechanical model of the lithosphere (crust and upper mantle) in Southern California using *UWGeodynamics* code (Moresi et al., 2002, 2003, 2007; Beucher et al., 2019). The model consists of a 3-D Cartesian domain that includes a longitudinal range of 113°W to 121°W, a latitudinal range of 31°N to 35°N, and a maximum lithosphere depth of 100 km (Figure 6), which is solved by 80 × 40 × 100 Eulerian nodes on a finite-element mesh with a resolution of 0.2° x 0.2° x 1km. We use a free-slip boundary condition at the top. We apply the Pacific-North America velocity boundary condition. We define an air and sticky-air layer on top of the surface topography to simulate the free surface. We also incorporate the thermal state of the model, as constrained from the seismic data in the mantle (Shen and Ritzwoller, 2016) and from published data products for the crust (Shinevar et al., 2018). Our 3-D model is based on visco-plastic materials. The strength of the crust and mantle are represented by a non-Newtonian rheology, a combination of viscous and plastic rheology (Figure 5).

(A)

Material	Density (kg/m³)	Heat capacity (J/°K.kg)	Heat diffusivity (m²/s)	Radiogenic heat production (pW/m³)	Flow law (dislocation creep)
Topography	2500	1000	8.3×10^{-7}	0.5	Wet Quartz (Gleason and Tullis, 1995)
Oceanic crust	2950	1000	1×10^{-6}	0.5	Dry Maryland Diabase (strong) (Burov, 2011)
Upper crust	2700	1000	8.3×10^{-7}	0.9	Wet Quartz (Gleason and Tullis, 1995)
Middle crust	2900	1000	6.7×10^{-7}	0.9	Wet Diorite (Carter and Tsenn, 1987)
Lower crust	2900	1000	6.3×10^{-7}	0.9	Dry Maryland Diabase (strong) (Burov, 2011)
Mantle lithosphere	3330	1000	1×10^{-6}	0.022	Dry Olivine (Burov, 2011)
Air	1	100	1×10^{-6}	0.0	1.0×10^{20} Pa s
Sticky air	1	100	1×10^{-6}	0.0	5.0×10^{18} Pa s
Water	997	1000	1×10^{-6}	0.0	5.0×10^{18} Pa s

(B)

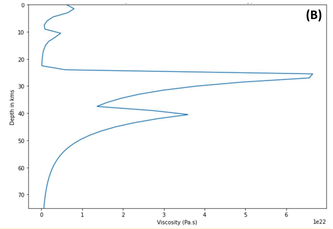

Figure. 5 *(A) Rheological parameters applied in thermomechanical model. (B) Strength profile formed from rheological parameters applied in the thermomechanical model.*

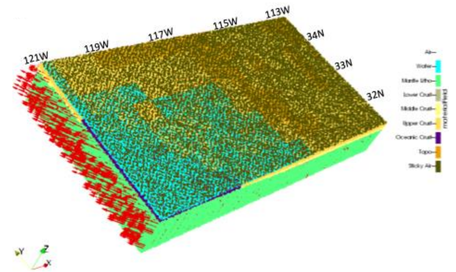

Figure 6. *3-D lithosphere structure model produced with the UWGeodynamics code and the kinematic boundary conditions in southern California. The model encompasses latitudes 31 °N to 35 °N, longitudes 113 °W to 121 °W and from 10km above sea level to 100km below sea level.*

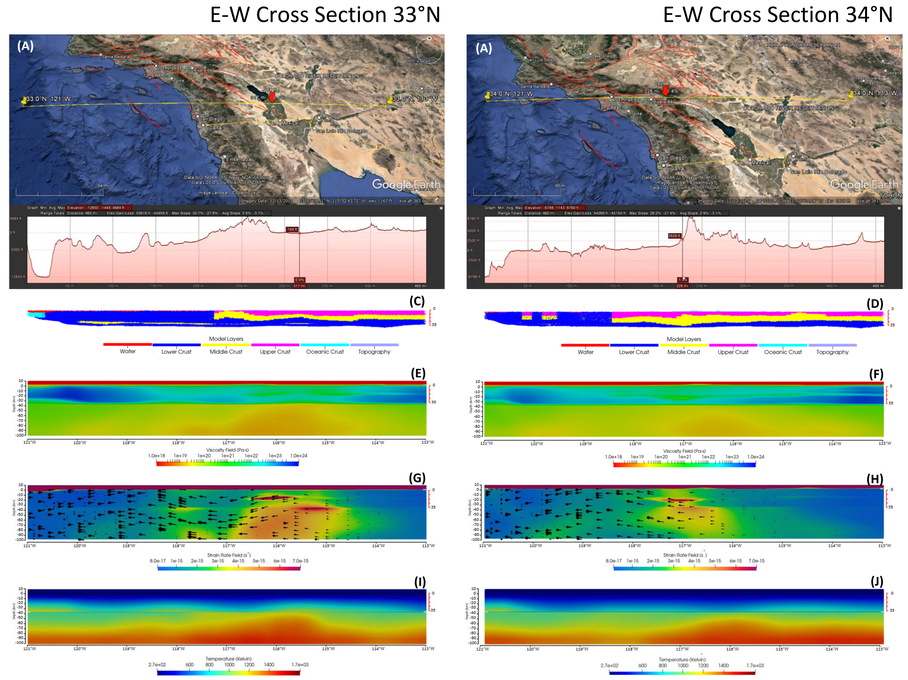

Figure. 7 *2-D, E-W cross sections through the 3-D model. Left column is cross section at 33 °N and the right column is at 34 °N. (A) Google map image of the cross section at 33 °N with elevation. (B) Google map image of the cross section at 34 °N with elevation. (C) Crustal layer structure at 33 °N. (D) Crustal layer structure at 34 °N. (E) Viscosity field at 33 °N. (F) Viscosity field at 34 °N. (G) Strain rate field with velocity vectors at 33 °N. (H) Strain rate field with velocity vectors at 34 °N. (I) Temperature field at 33 °N. (J) Temperature field at 34 °N.*

Results

- We use the 2-layer H-k stacking method to derive the Moho depth and crystalline crust Vp/Vs with eliminating the effects from the sedimentary layer.
- The crystalline crust Vp/Vs results are combined with the crustal Vs model to derive the abundance of SiO_2 wt% using an empirical relationship.
- Where the felsic composition exists at greater depths (wet diorite rheology [Carter and Tsenn. 1987]), horizontal lenses of relatively low crustal viscosity develop within middle and lower crustal depths.
- These low viscosity lenses often constitute zones of higher strain rates and play a role in the location of transform shear zones that accommodate plate motion.
- Both mantle temperature anomalies and lower viscosity zones in the lower crust are sights of vertical gradients of vertical motion and hence, possible lower crustal flow.

Acknowledgements

We thank SCEC (Award #21177), NSF-OPP-1945856, NSF EAR- 1814051 and EAR-202579 for funding.

References

- Andreas Plesch, et al. Community Fault Model (CFM) for Southern California Bulletin of the Seismological Society of America December 2007 97:1793-1802; doi:10.1785/0120050211
- B. R. Hacker, P. B. Kelemen, M. D. Behn, Continental lower crust, Annu. Rev. Earth Planet. Sci. (2015) 43:167–205.
- Brocher, T. M. Bulletin of the Seismological Society of America, Vol. 95, No. 6, pp. 2081–2092, December 2005, doi: 10.1785/0120050077
- Burov, E.B., (2011). Rheology and strength of the lithosphere. Marine and Petroleum Geology, 28 (8), 1402-1443.
- Carter, N.L. and Tsenn, M.C., (1987). Plow properties of continental lithosphere. Tectonophysics, 136: 27-63.
- Christensen N.I., (1996) Poisson's ratio and crustal seismology, J. Geophys. Res. 101, 3139-3156
- Gleason, G. C., & Tullis, J. (1995). A flow law for dislocation creep of quartz aggregates determined with the molten salt cell. Tectonophysics, 247(1-4), 1-23.
- Moresi, L., Dufour, F. & Mühlhaus, H. B. A Lagrangian integration point finite element method for large deformation modeling of viscoelastic geomaterials. *J. Comput. Phys.* 184, 476–497 (2003).
- Moresi, L., Dufour, F. D. R. & Hlhaus, H. B. M. Mantle convection modeling with viscoelastic/brittle lithosphere: numerical methodology and plate tectonic modeling. *Pure Appl Geophys* 159, 22 (2002).
- Moresi, L., Quenette, S., Lemiale, V., Meriaux, C., Appelbe, B. & Mühlhaus, H.B. Computational approaches to studying non-linear dynamics of the crust and mantle. *Phys. Earth Planet. Inter.* 163, (2007).
- Shen, W., and M. H. Ritzwoller (2016), Crustal and uppermost mantle structure beneath the United States, J. Geophys. Res. Solid Earth, 121, 4306–4342.
- Shinevar, W.J., Behn, M.D., Hirth, G. and Jagoutz, O., 2018. Inferring crustal viscosity from seismic velocity: Application to the lower crust of Southern California. *Earth and Planetary Science Letters*, *494*, pp.83-91.
- W. L. Yeck, et al., Sequential H-κ Stacking to Obtain Accurate Crustal Thicknesses beneath Sedimentary Basins, Bulletin of the Seismological Society of America, Vol. 103, No. 3, pp. 2142–2150, June (2013).
- Zhu, L., and H. Kanamori, Moho depth variation in southern California from teleseismic receiver functions, J. Geophys. Res., 105 (B2), 2969–2980, (2000).